

SHEAR-FLEXURAL INTERACTION IN ANALYSIS OF REDUCED WEB SECTION BEAMS USING VM LINK ELEMENT

S. Erfani, M. T. Kazemi*

Department of Civil Engineering, Sharif University of Technology
P.O. Box 11365-9313, Tehran, Iran
sderfani@yahoo.com - Kazemi@sharif.edu

*Corresponding Author

(Received: July 13, 2006 - Accepted: March 18, 2007)

Abstract Reduced web section beams in shear-yielding moment-resistant steel frames are used for energy dissipating of earthquakes. The finite element analysis indicates that failure mode of these beams are governed by the combination of shear force and flexural moment. Therefore the analysis of frames with reduced web section beams needs consideration of shear-flexural interaction in those sections. In the present paper, modeling and analysis of reduced web section beams are investigated by using a special element which is called VM link element. The elastic and inelastic shear and flexural deformations and tangential stiffnesses in this link element are considered by using the multi-surfaces plasticity concept with dissimilar yield surfaces. The developed VM link element is examined for some reduced web section beams and it is shown that the results have a good agreement with the finite element results.

Keywords VM Link Element, Shear-Flexural Interaction, Multi-Surface Plasticity, Reduced Web Section Beams

چکیده تیرهای فلزی با جان سوراخ شده، در قاب های خمشی لرزه بر ساختمان برای استهلاک انرژی مورد استفاده واقع می شوند. کاربرد روش المان محدود نشان دهنده این است که ترکیب نیروی برشی و لنگر خمشی بر نحوه رفتار غیر الاستیک این تیر ها حاکم بوده و بنابراین لحاظ کردن اندر کنش نیروی برشی - لنگر خمشی در تحلیل چنین تیر هایی ضروری می باشد. در مقاله حاضر، مدل سازی و تحلیل این نوع تیر ها با استفاده از المان ویژه ای به نام المان رابط VM مورد بررسی قرار می گیرد. تغییر شکل های الاستیک و غیر الاستیک برشی و خمشی و همچنین سختی های مماسی در این المان، بر اساس ایده سطوح تسلیم چندگانه در تئوری پلاستیسیته وبا استفاده از سطوح تسلیم غیر متشابه مورد لحاظ واقع می شوند. المان رابط توسعه داده شده VM بر روی چند مورد از تیرهای با جان سوراخ شده استفاده شده و نتایج حاصله با نتایج حاصل از روش المان محدود مقایسه می شود که انطباق خوبی بین آن ها مشاهده می گردد.

1. INTRODUCTION

Reduced web section beams in shear-yielding moment-resistant steel frames have been studied in recent researches [1]. These beams are used in steel frames for energy dissipating by shear yielding of their reduced webs. In Figure 1, two common types of these beams are shown. In type (a), near both ends of the beam, the web has been reduced. This type is usually used in frames with a small gravity load and the frames mainly resist lateral seismic loads. In these frames, the reduction of the beam's web close to the ends does not affect

their ability to resist the gravity loads and the reduced section part could dissipate the earthquake energy demand by yielding. In type (b), the beam's web is reduced in the middle region. This type can be used in frames in which the gravity load is considerable. In these frames the gravity's shear force is usually small in the middle and so the web section may be reduced.

Halterman and Aschheim [1] using the finite element method, indicated that the failure mode of these beams are affected by a combination of shear force and flexural moment. Thus analysis of these beams needs consideration in regard to the shear-

flexural interaction in the reduced web zones. The VM link element, which was developed by Kazemi and Erfani [2] to model shear-flexural interaction could be employed for the reduced web zones, too. Kazemi and Erfani [2,3] examined the VM link element for modeling and analyzing of some type (a) reduced web section beams (Figure 1-a) and some link elements in eccentrically braced steel frames. Comparison with the finite element results showed the suitable nearness. In this paper, modeling of the beams with the reduced section at the center (Figure 1-b) using the improved VM link element will be presented.

2. INELASTIC FRAME ANALYSES

Inelastic analysis and design of structures has made a great progress due to the rapid development of computer hardware and software in the recent decades [4-6]. Common approach for modeling of inelastic behavior in the beam elements has been to adopt inelastic hinge formation at the beam's critical sections. A generalized plastic hinge, with zero length, accounting for interaction for axial, torsional and biaxial bending moments, based on multi-surfaces plasticity concept was presented by Powell and Chen [7]. By using a piecewise linearized yield surface and linear kinematic hardening rule for concentrated hinges, Krenk et al. [8] developed a formulation for displacement discontinuities with extension and rotation components. A method for the modeling of members with yielding under combined flexure and axial force in steel frames subjected to earthquake ground motions was presented by Kim and Engelhardt [9]. Their method has the capability of modeling plastic axial deformation and changes in the axial stiffness, based on isotropic and kinematic strain-hardening defined in axial-flexural space. Liew et al. [10-12] used the two-surface plasticity concept for considering the inelastic interaction between axial force and bending moment, too.

To consider the shear-flexural interaction, Ricles and Popov [13] developed a formulation for modeling links in the eccentrically braced steel frames (EBFs), based on multi-surfaces plasticity concept. The link beam had a nonlinear

hinge at each end, which consisted of uncoupled shear and flexural nonlinear subhinges. The finite element method for modeling of the shear-flexural inelastic zones could also be used, but it may take extensive time and is not applicable. Saritas and Filippou [14] investigated the shear-flexural interaction in the link beams by using a displacement field based on Timoshenko's beam theory and integration of the biaxial stress-strain relations over several control sections along the beams. Each control section subdivided into several layers. This method is a general way of considering axial, shear and flexural interaction in the frames. Although predicted behavior shows a good accuracy, because of integration in several points, it is time consuming. Kazemi and Erfani [2,3,15] proposed the VM link element for use in frames where shear-flexural interaction should be considered. The element can be used in any arbitrary location of the frames and may have zero or a nonzero length. The multi-surface concept with dissimilar yield surfaces was adopted. In the present paper, a new improved revision of the VM link element is briefly described and is employed for modeling of the reduced web section beams type b (Figure 1-b).

3. DEFINITION OF THE VM LINK ELEMENT

The introduced VM link element includes one inner inelastic hinge with zero length and two rigid beams with zero or nonzero lengths in two sides of it. As seen in Figure 2, *i* and *j* are the outer nodes and *h* is the inner hinge which has an arbitrary location. The lengths of the two rigid parts are L_i and L_j , and $L = L_i + L_j$ is the total length of the element. The inelastic zones of beams could be modeled by this link element.

If the link's end forces and displacements are described as column matrixes of P and U , respectively (see Figure 3a) and the element's internal forces and deformations in the inner inelastic hinge are defined as column matrixes of P_h and U_h , respectively (see Figure 3b). Then one could express:

$$P = AP_h \quad (1)$$

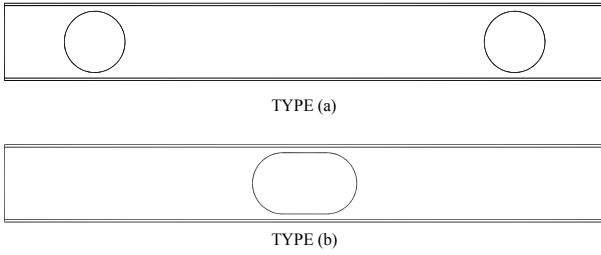


Figure 1. Two common types of reduced web section beams.

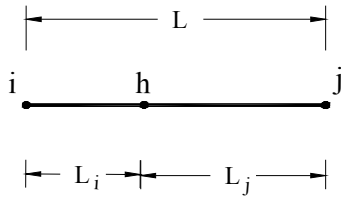


Figure 2. Geometrical configuration of the VM link element.

$$U_h = A^T U \quad (2)$$

where A is the transformation matrix, which its components depend only on the lengths of the rigid parts of the link and are as follows:

$$A = \begin{bmatrix} A_i \\ A_j \end{bmatrix} = \begin{bmatrix} -1 & 0 & 0 \\ 0 & -1 & 0 \\ 0 & -L_i & -1 \\ 1 & 0 & 0 \\ 0 & 1 & 0 \\ 0 & -L_j & 1 \end{bmatrix} \quad (3)$$

It is assumed that no loads or masses are assigned to the hinge and to the rigid parts except at the end nodes. The element's tangential stiffness matrix K can be related to K_h and F_h as:

$$K = AK_h A^T = AF_h^{-1} A^T \quad (4)$$

where K_h and F_h are the tangential stiffness and

flexibility matrixes of the inner hinge, respectively.

4. INNER HINGE'S FLEXIBILITY AND STIFFNESS

If the rates of forces and deformations in the element's inner hinge are shown as \dot{P}_h and \dot{U}_h , respectively, then one could write:

$$\dot{P}_h = K_h \dot{U}_h \quad (5)$$

The components of K_h can be obtained by inverting the inner hinge's tangential flexibility matrix, F_h . For the small deformation, F_h can be decomposed as:

$$F_h = F_h^e + F_h^p \quad (6)$$

where F_h^e and F_h^p are the inner hinge's elastic and plastic tangential flexibility matrixes, respectively. The components of F_h^e may be obtained from the classic formulas and F_h^p is assumed as:

$$F_h^p = \varphi_V F_{hV}^p + \varphi_M F_{hM}^p \quad (7)$$

In which F_{hV}^p and F_{hM}^p are the flexibility matrixes related to the pure shear and the pure flexural loadings, respectively. φ_V and φ_M are arbitrary functions satisfying the conditions of $\varphi_V = 1$, $\varphi_M = 0$ for the pure shear loading and $\varphi_V = 0$, $\varphi_M = 1$ for the pure flexural loading. In the present study, φ_V and φ_M are supposed as:

$$\varphi_V = m_V^2 (1 + (a_V - 1)(1 - m_V^2)) \quad (8)$$

$$\varphi_M = m_M^2 (1 + (a_M - 1)(1 - m_M^2)) \quad (9)$$

where m_V and m_M are the components of m vector,

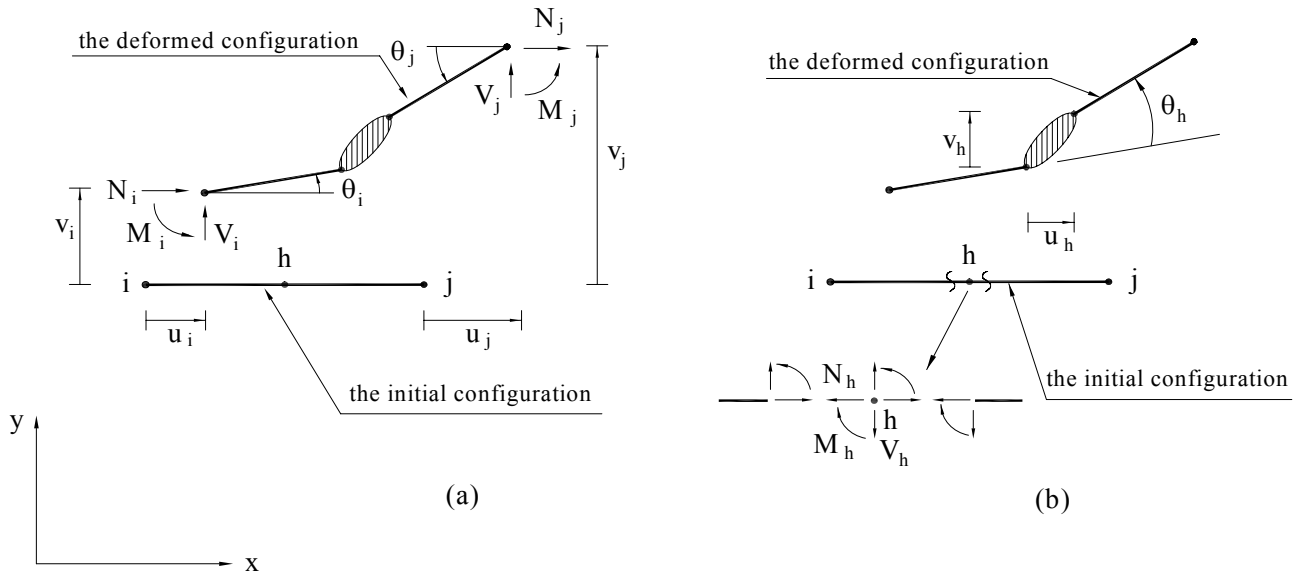


Figure 3. (a) The element's end forces and displacements, (b) The element's internal forces and deformations.

which is the unit location vector of the action point in VM space (See Figure 4). The a_v and a_M are constant parameters which depend on the joint geometry, size and material. Using them, the flexibility may be decreased through combining of shear and flexure. The results of the experimental studies or the numerical analyses may be used for determination of F_{hV}^D , F_{hM}^D , a_v and a_M . In the current paper, they are obtained through using the finite element analysis.

Equation 7 implies that the flow rule is not associated. For non-associated plasticity, to differentiate between plastic flow and elastic unloading, the loading-unloading criteria need to be defined more precisely. Suppose the action point lies on a yield surface and the deformation rate is \dot{U}_h . The first step is to take $K_h = (F_h^e)^{-1}$, the action rate \dot{P}_h is then predicted. If the condition $\lambda_1 = n^T \dot{P}_h < 0$ was observed, it means that we have unloading and for the condition $\lambda_1 = 0$, the natural loading is governed.

For the corner points, these conditions for

both n_B and n_C should be satisfied. n_B and n_C are the unit normal vectors at points B and C, which are very close to the corner, but on two different surfaces (see Figure 4).

If the condition $\lambda_1 > 0$ was encountered, using $K_h = (F_h^e + F_h^D)^{-1}$, the new action rate \dot{P}_h is calculated using Equation 5. With the new \dot{P}_h , if the condition $\lambda_2 = n^T \dot{P}_h > 0$ is reached, the plastic loading condition will govern. For the corner point, plastic loading condition needs to be satisfied only for one of the unit vectors, n_B or n_C . If $\lambda_2 \leq 0$, the stiffness matrix will be adjusted to:

$$K_h = (F_h^e + F_h^D)^{-1} - \frac{\lambda_2}{\lambda_1} (F_h^e)^{-1} \quad (10)$$

By using the adjusted stiffness and calculating the new action rate \dot{P}_h (normality condition) $n^T \dot{P}_h = 0$ will reach and the natural loading conditions will govern.

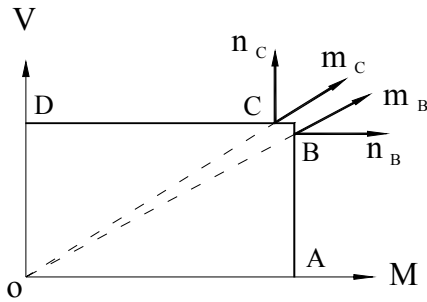


Figure 4. The normal and location vectors at a corner point.

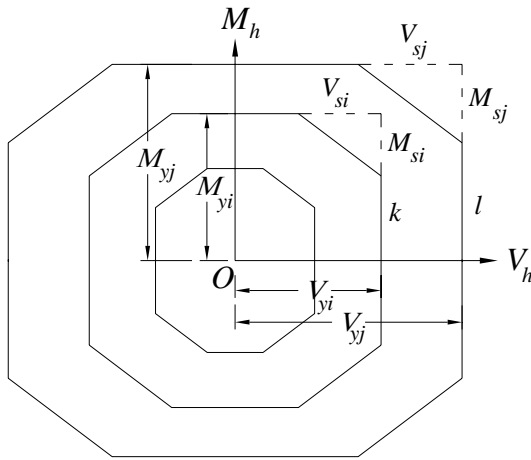


Figure 5. Polygonal dissimilar yield surfaces.

5. YIELD SURFACES

For considering interaction between the shear force and flexure, the multi-surface concept in shear-flexural space is used (see Figure 5). This concept, which was originally defined in stress space [16,17], was adapted with some modifications for the resultant forces space for the frame elements [7-14].

It is assumed that the yield surfaces are convex and could be translated and changed in size. They could not be intersected, but could be tangential to each other. If the action point is in the internal part of initial yield surface, the behavior will be elastic and if it is on each of the surfaces, the behavior will be elastoplastic. In tangency of several yield surfaces, the outer surface properties define the

current behavior. The similarity assumption among yield surfaces has been used in most works in regard to having parallel normal directions for the corresponding points on the yield surfaces. If it is assumed in the shear-flexural space that the yield surface i is similar to the yield surface j , then we will have:

$$\frac{V_{yi}}{V_{yj}} = \frac{M_{yi}}{M_{yj}} \quad (11)$$

where V_{yi} , V_{yj} , M_{yi} and M_{yj} are the points on i and j yield surfaces for the pure shear and flexural loadings. In general, this may not be a suitable assumption and the pure flexural yielding is very different from pure shear yielding. In the present research, with dissimilar polygonal yield surfaces shown in Figure 5, the shear-flexural interaction is considered more realistically. To prevent intersection of the yield surfaces, the corresponding sides of all yield surfaces should be parallel with each other and the length of any side of any yield surface should be smaller than the length of the corresponding side of the next outer yield surface. For the yield surfaces presented in Figure 5, the conditions of $V_{si} \leq V_{sj}$, $M_{si} \leq M_{sj}$, $V_{yi} - V_{si} \leq V_{yj} - V_{sj}$, and $M_{yi} - M_{si} \leq M_{yj} - M_{sj}$ must be ensured. Also, in order to keep parallel the corresponding sides of the yield surfaces with each other, we should have:

$$\frac{V_{si}}{V_{sj}} = \frac{M_{si}}{M_{sj}} \quad (12)$$

6. HARDENING RULE

All of the yield surfaces may move, except the last yield surface, which is fixed and presents the plastic capacity of the hinge. In some recent works [7-14], the element formulation is based on combined kinematic and isotropic hardening rules for shear force and only a kinematic hardening rule for the flexural moment. In this paper, only kinematic hardening is used for both the shear and flexure, although isotropic hardening could be

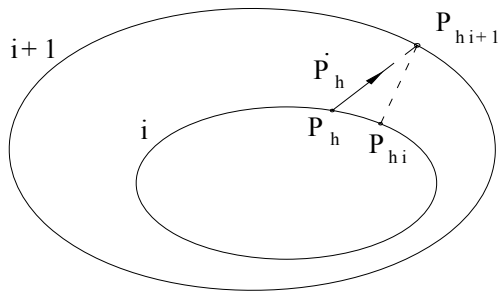


Figure 6. Action point and corresponding points on two adjacent yield surfaces.

implemented, too.

For managing the yield surfaces, the kinematic hardening rule, which was recently proposed by Kazemi and Erfani [2,3] is used. The i -th yield function is defined as:

$$\phi_i(P_h - \alpha_i) = 0 \quad (13)$$

where P_h is the action vector of the inner hinge and α_i is the i -th yield function center. If the action location is on the i -th yield surface and plastic loading occurs, the rate of i -th yield surface translation, $\dot{\alpha}_i$, may be defined as:

$$\dot{\alpha}_i = (P_{hi+1} - P_{hi}) \dot{\mu} \quad (14)$$

where, P_{hi+1} is the intersection point between the direction of the action rate, \dot{P}_h , and $(i+1)$ -th yield surface. The term P_{hi} is the conjugate point of P_{hi+1} on i -th yield surface (see Figure 6).

By this definition, when the action point, P_h , approaches closer to $(i+1)$ -th yield surface, i -th yield surface moves, in a way that the two points on the i -th yield surface, P_{hi} and P_h , approach closer to each other and coincide with P_{hi+1} , asymptotically. Then the inner moving yield surface may be tangential to the outer yield surface at the contact point and they never intersect. To calculate $\dot{\mu}$, plastic loading

condition ($\dot{\phi}_i = 0$) is used, hence:

$$\dot{\mu} = \frac{\frac{\partial \phi_i}{\partial P_h} \dot{P}_h}{\frac{\partial \phi_i}{\partial P_h} (P_{hi+1} - P_{hi})} \quad (15)$$

By substituting Equation 15 in Equation 11, $\dot{\alpha}_i$ can be demonstrated that:

$$\dot{\alpha}_i = \frac{\frac{\partial \phi_i}{\partial P_h} \dot{P}_h}{\frac{\partial \phi_i}{\partial P_h} (P_{hi+1} - P_{hi})} (P_{hi+1} - P_{hi}) \quad (16)$$

$\dot{\alpha}_i$ is the translation rate for i -th yield surface, due to loading

7. REDUCED WEB SECTION BEAM

A reduced web section beam as shown in Figure 7 is investigated. The beam consists of W21× 68 section ($A = 13131 \text{ mm}^2$, $I = 625770000 \text{ mm}^4$, and $A_s = 5900 \text{ mm}^2$) with the span length of 4000 mm and only one hole at the center, where A , I and A_s are the area, the moment of inertia and the shear area of the beam section. The geometry of the hole is presented in Figure 7. Multi-linear kinematic hardening plasticity is assumed for the material of the beam, with $F_y = 360 \text{ MPa}$, $F_u = 500 \text{ MPa}$, $E = 200 \text{ GPa}$, $H = 0.005E$ and $\nu = 0.3$, where F_y and F_u are the yield and ultimate stress, E and H are the initial and the post yield moduli and ν is the Poisson ratio, respectively.

For the modeling of the central part of the beam, a VM link element with length of $L = 1260 \text{ mm}$ is used. Location of the inner hinge is assumed in the middle of the VM element ($L_i = L_j = 630 \text{ mm}$), coinciding with the center of the hole, as shown in Figure 8.

For determination of the VM link element's parameters, the beam's middle part with a length of 1260 mm and containing the hole is analyzed for pure shear and pure flexural, separately. In the pure shear loading, the flexural moment is zero and for

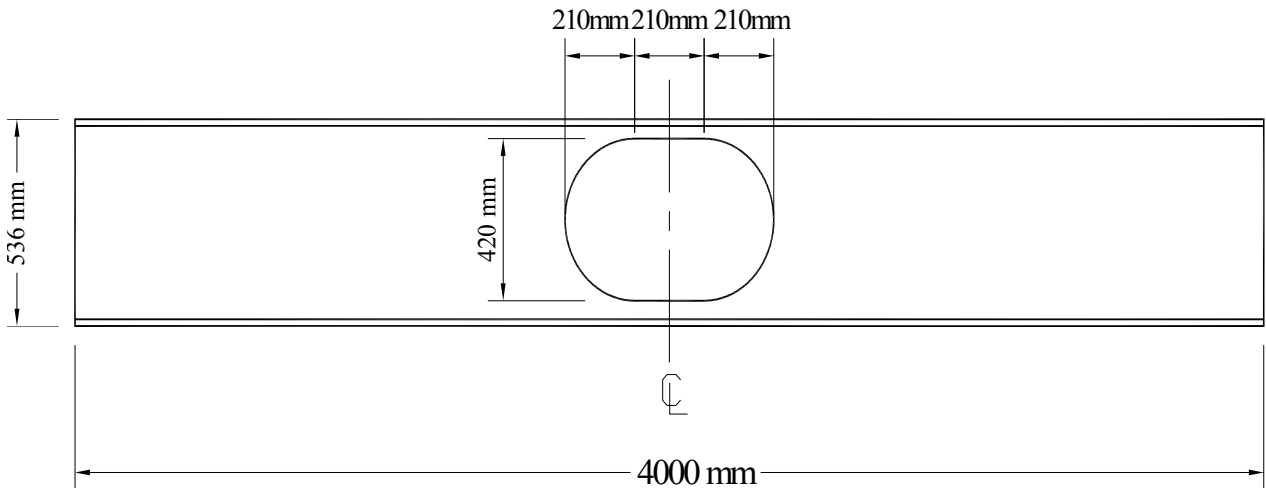


Figure 7. Two common types of reduced web section beams.

the pure flexural loading, the shear force is zero at the hole's center (see Figure 9).

The analyses are performed by the nonlinear finite element software, ANSYS, using solid element SOLID45. The Results are presented in Figure 10, where extracted yield points are shown.

In the figures, the horizontal axes indicate the displacement and rotation of the right end. Based on the results, the yield surfaces for the inner hinge are simplified as shown in Figure 11 and Table 1.

The inner hinge flexibility matrixes in between the two consecutive yield surfaces may be calculated as:

$$F_h^* = A_j^T F_{jj} A_j \quad (17)$$

Where A_j defined from Equation 3 with assumption of $L_j = 630$ mm and F_{jj} is the element at node j as follows:

$$F_{jj} = \begin{bmatrix} \frac{1}{r_0} \frac{L}{EA} & 0 & 0 \\ 0 & \frac{1}{k_1} \frac{1}{r_1} \frac{L^3}{3EI} + \frac{1}{k_2} \frac{1}{r_2} \frac{L}{GA_s} & \frac{1}{k_3} \frac{1}{r_3} \frac{L^2}{2EI} \\ 0 & \frac{1}{k_3} \frac{1}{r_3} \frac{L^2}{2EI} & \frac{1}{k_4} \frac{1}{r_4} \frac{L}{EI} \end{bmatrix} \quad (18)$$

$r_0, r_1, r_2, r_3,$ and r_4 are the equivalent effective stiffness factors. From the finite element analysis the values of 0.862, 0.955, 0.108, 0.955, and

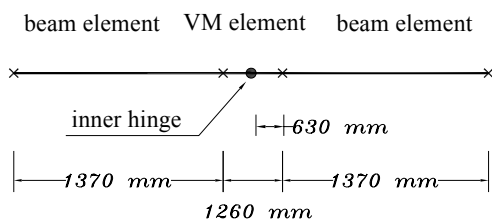


Figure 8. Modeling of the reduced web section beam with beam and the VM link elements.

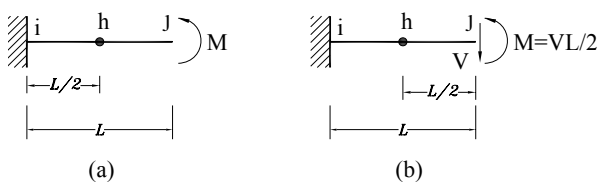


Figure 9. Boundary conditions and loadings of the VM link element for (a) pure flexural and (b) pure shear.

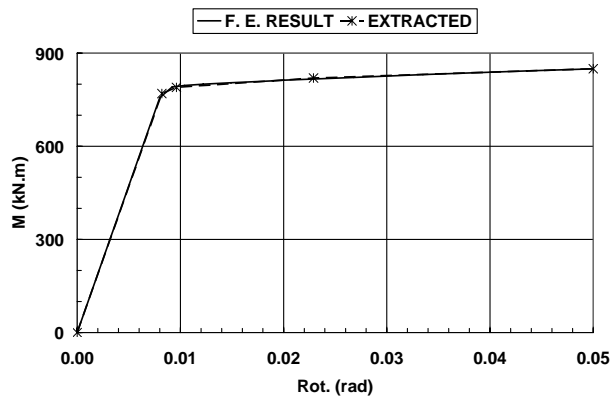
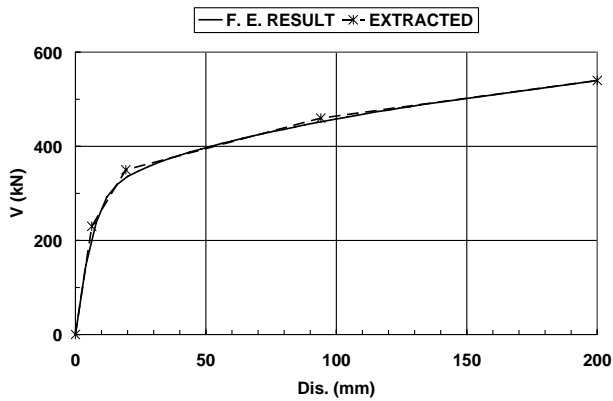


Figure 10. Finite element results and extracted yield points in pure loadings.

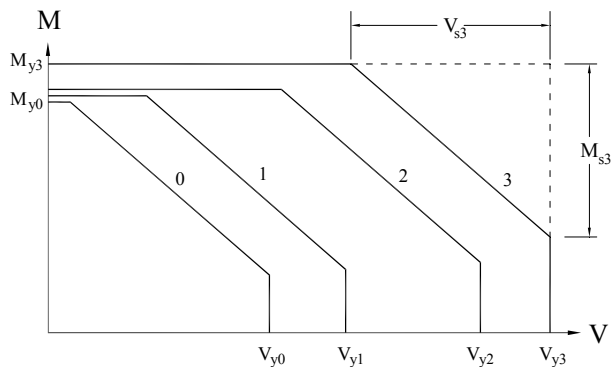


Figure 11. The inner hinge yield surfaces.

0.955, are obtained, respectively. k_1 , k_2 , k_3 and k_4 are the hardening coefficients. If we assume that

$k_1 = k_2 = k_3 = k_4 = 1$, the F_h^* will change to F_h^e , and if the coefficients are selected as appropriate value for pure loadings, as presented in Table 2, the F_h^* will change to F_{hV}^D or F_{hm}^D . After the calculation of F_h^e , F_{hV}^D and F_{hm}^D , using Equations 17 and 18, the total flexibility matrix, F_h , is obtained from Equations 6 and 7. For definition of the a_V and a_M , used in Equation 7, combined shear force and flexural moment at the inner hinge location should be applied. The middle part of the beam was reanalyzed by the finite element method for a combined loading and the a_V and a_M were resulted, as shown in Table 2.

8. INELASTIC ANALYSIS USING VM LINK ELEMENT

The beam shown in Figure 7 is analyzed for three different boundary conditions and loadings. The analyses are performed using the finite element method (ANSYS software), and VM link element modeling, and their main results are compared.

In the first example, rotational freedoms at the both ends are prevented and the right end of the beam is subjected to a cyclic displacement, as shown in Figure 12. The shear force at the inner hinge location resulted from the finite element method and VM link element modeling is compared in Figure 13. As seen, the results have excellent agreement with each other. It is noted that, the flexural moment at the inner hinge location is zero in this case and the shear yielding is the governing mode.

In the second example, the rotational freedom at the right end of the beam is released and the right end of the beam is subjected to a cyclic displacement, as shown in Figure 12. The comparison between the finite element method and the VM link element modeling are presented in Figure 14. As seen, the results have a good agreement with each other.

The translation of yield surfaces for the inner hinge of the VM link element is shown in Figure 15. As seen, the action point is located at the shear-flexural interaction zone.

For the third example, the displacement

TABLE 1. The Inner Hinge Yield Surfaces Parameters.

YieldSurfaces	V_{yi} (kN)	M_{yi} (kN. m)	V_{si} (kN)	M_{si} (kN. m)
$i = 0$	230	770	161	375
$i = 1$	350	790	169	394
$i = 2$	460	820	177	413
$i = 3$	540	850	185	431

TABLE 2. The Inner Hinge Flexibility Matrixes Parameters.

Between Yield Surfaces:	K_1, K_2, K_3 and K_4		a_V and a_M	
	Pure Shear	Pure Flexural	Pure Shear	Pure Flexural
0 and 1	0.250	0.150	3.0	3.0
1 and 2	0.040	0.024	2.5	2.5
2 and 3	0.020	0.012	2.0	2.0

freedom at the right end of the beam is prevented and the right end of the beam is subjected to a cyclic rotation, as shown in Figure 16. The comparison between the results of finite element method and the VM link element modeling is presented in Figure 17. As seen, the results have fairly good agreement with each other. The translation of yield surfaces for the inner hinge of the VM link element is shown in Figure 18. As seen, the shear yielding is governed, at the beginning, but later the action point moves to the shear-flexural interaction zone. Comparison of the results in the three cases yielded that, although the failure modes are different, the VM link element modeling has good accuracy.

9. CONCLUSIONS

In this paper, analysis of the reduced web section beams was investigated. The reduced web section beams are used for earthquake energy

dissipation in shear-yielding moment-resistant steel frames. The shear-flexural interaction in the reduced web zones was modeled by the proposed VM link element. The elastic and inelastic shear and flexural deformations and tangential stiffnesses in this element, are considered by using the multi-surfaces approach with dissimilar yield surfaces. The VM link element was examined for some reduced web section beams and it was shown that the results of analysis using VM link element, which requires less computer time, have good agreement with the finite element results.

10. REFERENCES

1. Halterman, A. and Aschheim, M., "Analytical Studies of Shear-Yielding Moment-resistant Steel Frames", *12th World Conference on Earthquake Engineering*, Auckland, New Zealand, Paper No. 1544, (2000).
2. Kazemi, M. T. and Erfani, S., "Mixed Shear-flexural (VM) Hinge Element and It's Application", *Scientia*

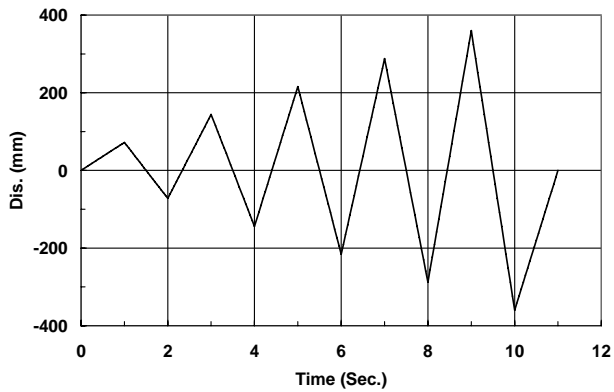


Figure 12. Relative displacement applied between two ends of the first and second example.

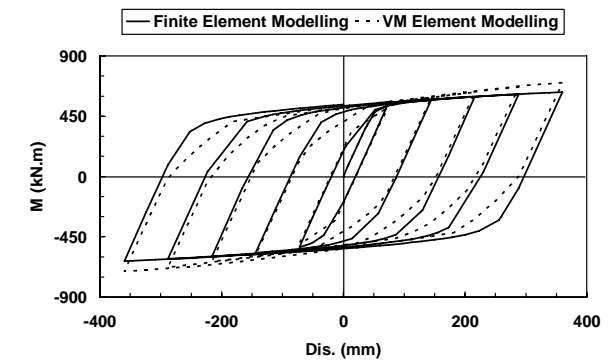
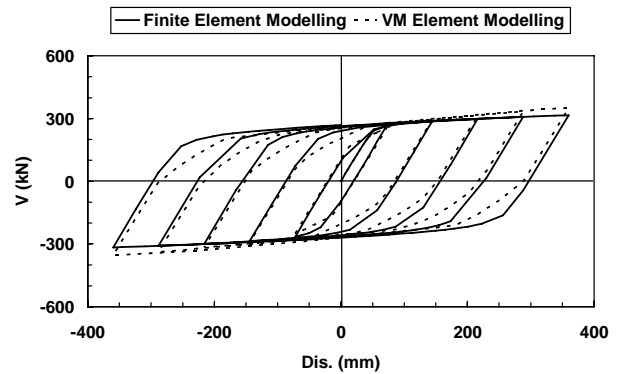


Figure 14. Comparison of results for the second example.

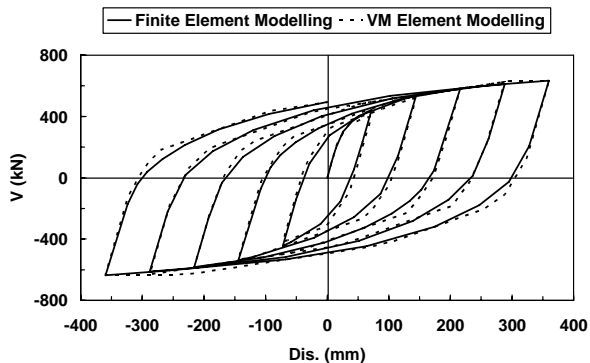


Figure 13. Comparison of results for the first example.

3. *Iranica*, Vol. 14, No. 3, (2007), 193-204.
3. Kazemi, M. T. and Erfani, S., "VM Link Element for Modeling of Shear-flexural Interaction in Reduced Web Section Beams", *Seventh International Congress on Advances in Civil Engineering, Istanbul, Turkey*, Paper No. ace 06-131 (2006).
4. Chen, W. F. and Lui, E. M., "Stability Design of Steel Frames", Boca Raton, FL: CRC Press, (1991).
5. Mazzolani, F. M. and Piluso, V., "Theory and Design of Seismic Resistant Steel Frames", E and FN Spon: hampion and Hall, (1996).
6. Jirasek, M. and Bazant, Z. P., "Inelastic Analysis of Structures", New York, John Wiley and Sons: LTD (2002).
7. Powell, G. H. and Chen, P. F. S., "3D Beam-Column Element with Generalized Plastic Hinges", *ASCE Journal of Engineering Mechanics*, Vol. 112, No. 7, (1986), 627-641.
8. Krenk, S., Vissing, S. and Vissing, J. C., "A Finite Step

- Updating Method for Elastoplastic Analysis of Frames", *ASCE Journal of Engineering Mechanics*, Vol. 119, No. 12, (1993), 2478-2495.
9. Kim, K. D. and Engelhardt, M. D., "Beam-Column Element for Nonlinear Seismic Analysis of Steel Frames", *ASCE Journal of Structural Engineering*, Vol. 126, No. 8, (2000), 916-925.
10. Liew, J. Y. R. and Tang, L. K., "Advanced Plastic Hinge Analysis for the Design of Tubular Space Frames", *Engineering Structures*, Vol. 22, No. 7, (2000), 769-783.
11. Liew, J. Y. R., Chen, W. F. and Chen, H., "Advanced Inelastic Analysis of Frame", *Journal of Construction Steel Research*, Vol. 55, No. 3, (2000), 245-265.
12. Liew, J. Y. R., Chen, H., Shanmugam, N. E. and Chen, W. F., "Improved Nonlinear Plastic Hinge Analysis of Space Frame Structures", *Engineering Structures*, Vol. 22, No. 10, (2000), 1324-1338.
13. Ricles, J. M. and Popov, E. P., "Inelastic Link Element for EBF Seismic Analysis", *ASCE Journal of Structural Engineering*, Vol. 120, No. 2, (1994), 441-463.

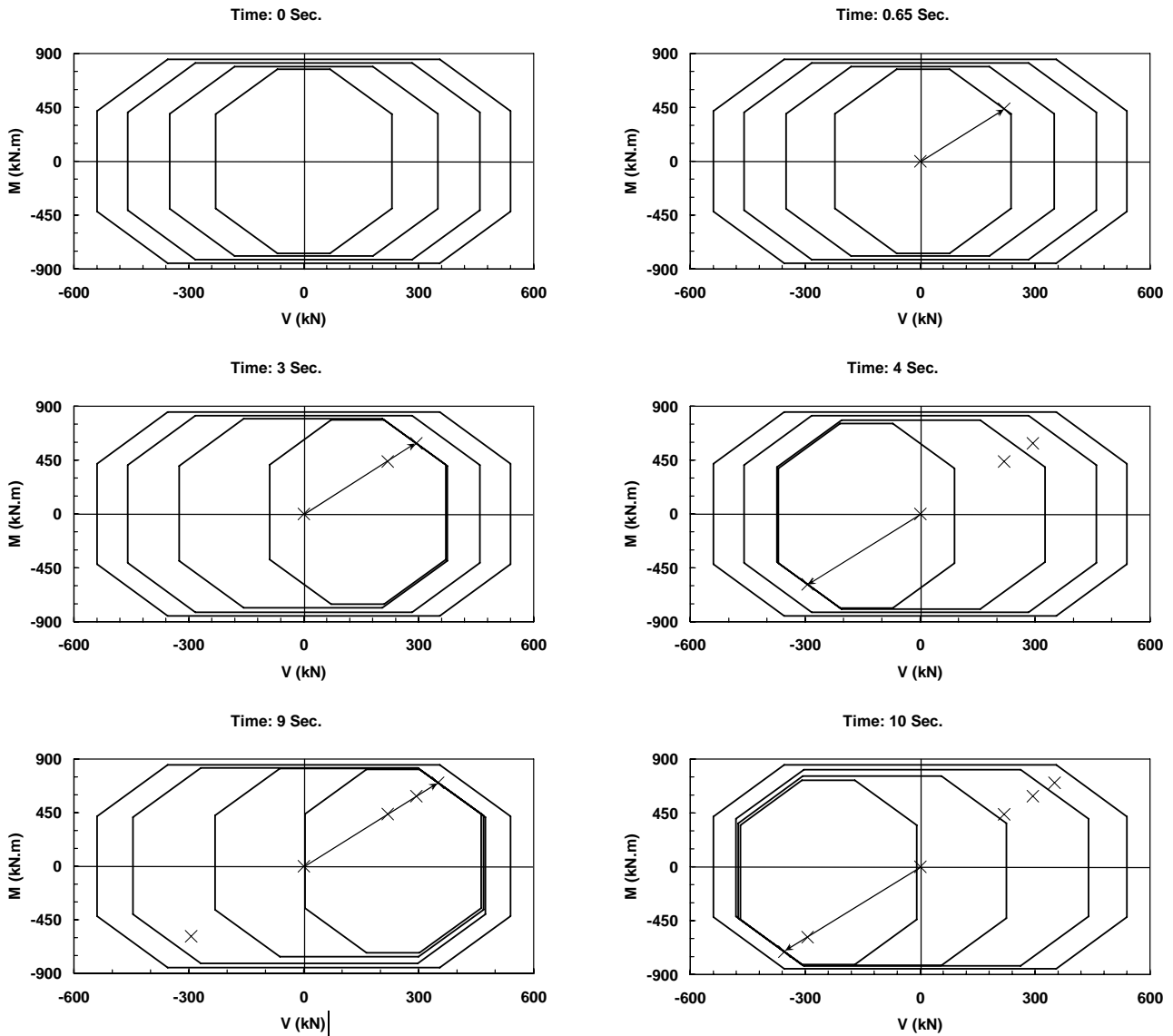


Figure 15. Translation history of yield surfaces for the inner hinge for the second example.

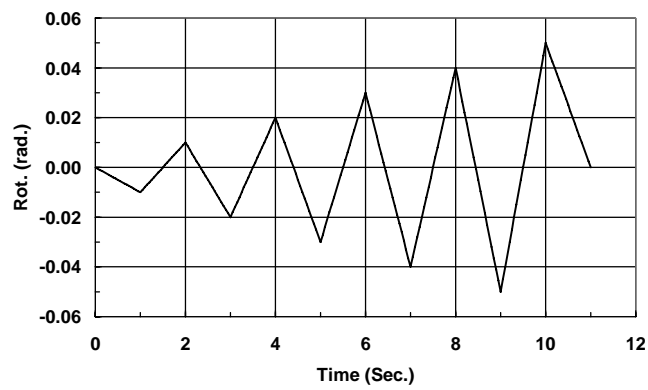


Figure 16. Cyclic rotation applied to right end of the beam for the third example.

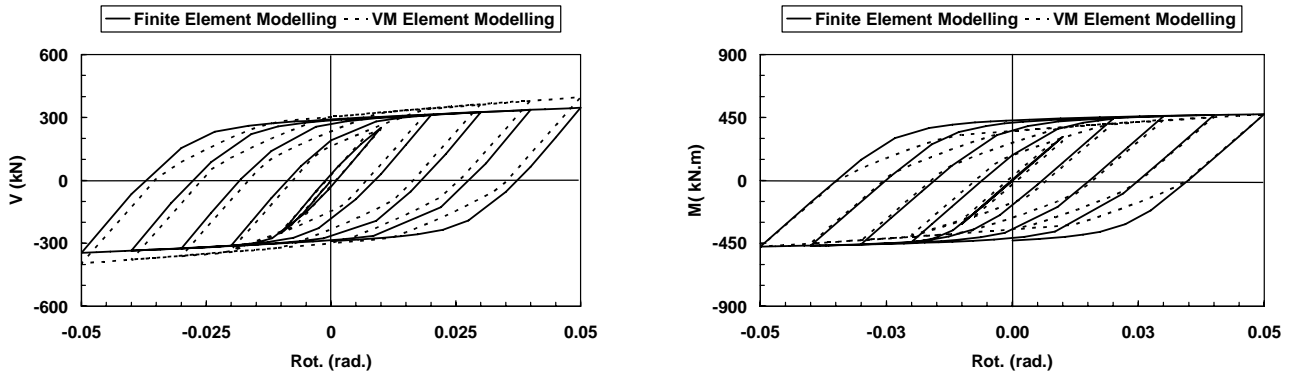


Figure 17. Comparison of results for the third example.

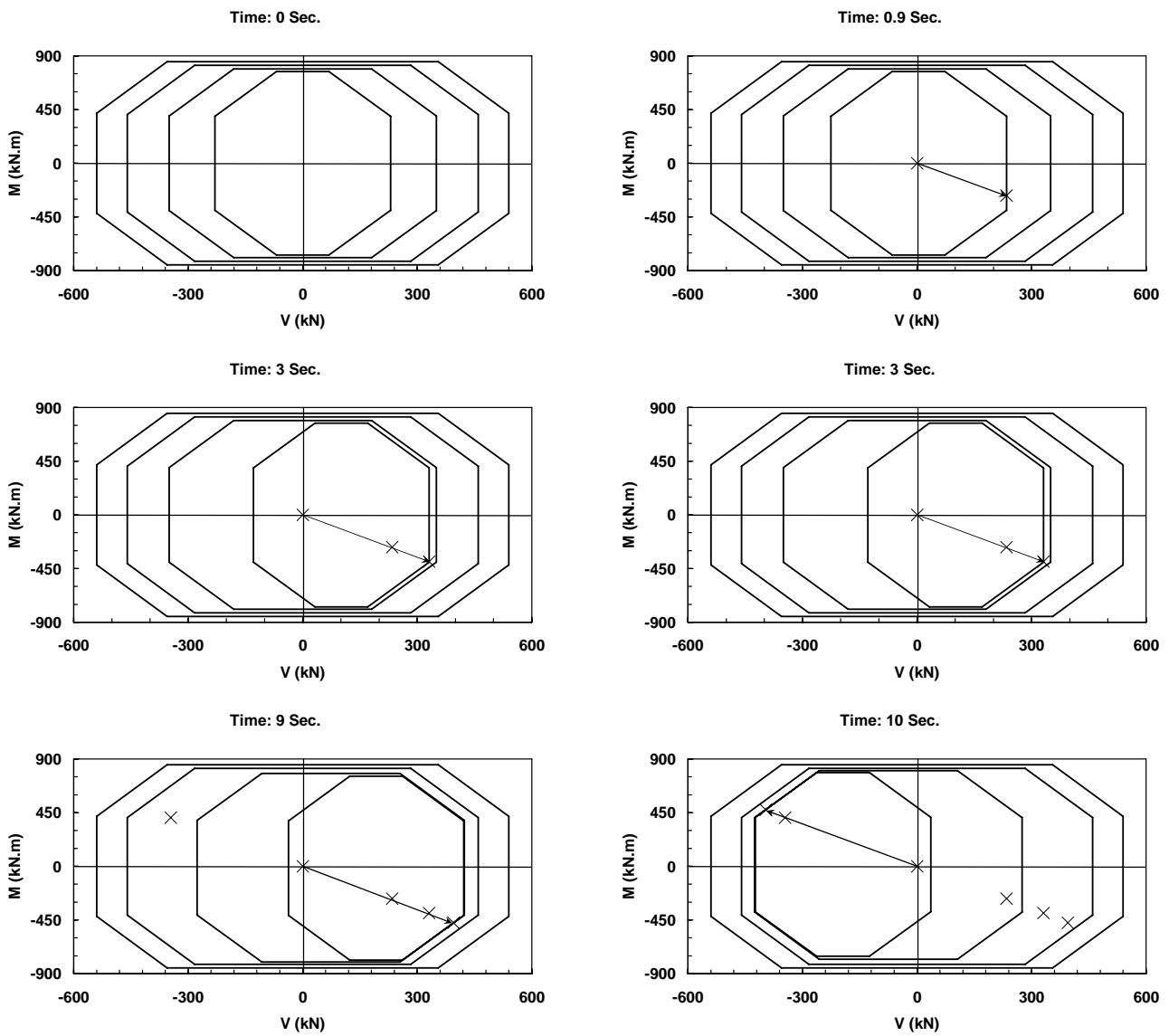


Figure 18. Translation history of yield surfaces for the inner hinge for the third example.

14. Saritas, A. and Filippou, F. C., "Modeling of Shear-yielding Members for Seismic Energy Dissipation", *13th World Conference on Earthquake Engineering*, Vancouver, Canada, Paper No. 1799, (2004).
15. Erfani, S. and Kazemi, M. T., "VM Link Element for Consideration of Shear-flexural Interaction", *The Tenth East Asia Pacific Conference on Structural Engineering and Construction*, Bangkok, Thailand, Vol. Analytical and Computational Methods, (2006), 149-154.
16. Khan, A. S. and Huang, S., "Continuum Theory of Plasticity", New York: John Wiley and Sons. Inc. (1995).
17. Mroz, Z., "An Attempt to Describe the Behavior of Metals Under Cyclic Loads Using a More General Workhardening Model", *Acta Mechanica*, Vol. 7, No. 2-3, (1969), 199-212.
18. Ramadan, T. and Ghobarah, A., "Analytical Model for Shear Link Behavior", *ASCE Journal of Structural Engineering*, Vol. 121, No. 11, (1995), 1574-1580.